Journal of Nano- and Electronic Physics
Vol. **15** No 5, 05002(4pp) (2023)

Журнал нано- та електронної фізики
Том **15** № 5, 05002(4cc) (2023)

Influence of Pressure on the Electronic and Magnetic Properties of the ZnSeTe Solid Solution Doped with Fe Atoms

S.V. Syrotyuk[1,*], M.K. Hussain[2]

[1] *Lviv Polytechnic National University, 12, S. Bandera st., 79013 Lviv, Ukraine*
[2] *AL-Hussain University College, Karbala-Najaf str., 56001 Kerbala, Iraq*

(Received 10 July 2023; revised manuscript received 18 October 2023; published online 30 October 2023)

First, this work examines the structural characteristics of the formation of a ZnSeTe solid solution. Further, after the introduction of Fe substitution impurity, electronic energy spectra and densities of electronic states were calculated. Significant changes in parameters of the electronic structure and magnetic properties caused by external hydrostatic pressure were revealed. It was found that the doped solid solution of ZnFeSeTe under normal conditions is a semiconductor for both spin orientations. However, under the action of hydrostatic pressure, this material turns into a metallic state, since the 3d states of iron are now at the Fermi level. Under the influence of pressure, the magnetic moment of the supercell decreases by more than six times, that is, from 4.0 to 0.67 Bohr magnetons.

Keywords: ZnSeTe solid solution, 3d impurity, Electronic energy bands, Magnetic moment, Pressure effect.

DOI: 10.21272/jnep.15(5).05002 PACS numbers: 71.15.Mb, 71.20.Nr, 71.27. + a

1. INTRODUCTION

Single crystals of ZnSeTe having uniform composition were grown on a ZnSe or ZnTe seed over the whole range of molar composition by a vapor-phase sublimation technique [1]. Measurable improvements in the purity of the final crystals were achieved by the slightly modified version of the simple vapor-phase sublimation technique, by which single crystals without ZnO inclusions were grown [1].

Optical characterization was performed on wafers sliced from crystals of ZnSe, ZnTe, and $ZnSe_{1-x}Te_x$ ($0 < x < 0.4$) grown by physical vapor transport [2]. Energy band gaps at room temperature were determined from optical transmission measurements on 11 wafers. A best fit curve to the band gap versus composition x data gives a bowing parameter of 1.45. This number lies between the value of 1.23 determined previously on ZnSeTe bulk crystals and the value of 1.621 reported on ZnSeTe epilayers. Low-temperature photoluminescence (PL) spectra were measured on six samples. The spectra of ZnSe and ZnTe were dominated by near band edge emissions and no deep donor-acceptor pairs were observed. The PL spectrum exhibited a broad emission for each of the $ZnSe_{1-x}Te_x$ samples, $0.09 < x < 0.39$. For $x = 0.09$, this emission energy is about 0.2 eV lower than the band gap energy measured at low temperature. As x increases the energy discrepancy gradually decreases and reduces to almost zero at $x = 0.4$. The single broad PL emission spectra and the spectra measured as a function of temperature were interpreted as being associated with the exciton bound to Te clusters because of the high Te content in these samples [2].

The optical parameters were obtained alone from the transmission spectrum of the $ZnSe_xTe_{1-x}$ thin films [3]. The thickness of the $ZnSe_xTe_{1-x}$ thin film is about 368.48 nm and the single-oscillator energy and the dispersion energy are about 3.64 and 17.19 eV, respectively. The value of optical band gap (≈2.34 eV) for the thin films in a direct transitions type was determined by the analysis of absorption data. The difference in the band gap between the bulk and film might be due to the strain and temperature effects [3].

In case of ZnSe (Te, O), the combination of semiconductor properties and characteristics of a highly efficient scintillator makes it possible to create scintielectronic detectors of X-ray radiation. But at higher energies' use of ZnSe(Te, O) is limited by bad transparence and also the high value of refractive index ($n = 2.4$) which leads to significant light losses. To overcome this problem combined X-ray detectors based of semiconductor-scintillator ZnSe (Te, O) were suggested. Detectors of charged particles and ultraviolet radiation based on the Schottky barrier structure of "metal-nZnSe(Te)" have also been developed. ZnSe(Te) have also been found useful for advanced medical application of computer X-ray tomography. Computer X-ray tomography is a powerful tool for early recognition of various diseases, especially those requiring surgery. Hence, ZnSe(Te) crystals can be used in low energy detectors in computer X-ray tomography [4].

We analyze physical models accounting for deep-level conduction band transitions to describe impurity absorption spectra in tetrahedral-structured semiconductors [5]. The investigations were carried out for ZnSe crystals doped with transition metals (Ti, V, Cr, Mn, Fe, Co, Ni) from a vapor phase. It was shown that the impurities provide acceptor centers with ground state energy offset by 0.3-0.6 eV from the edge of the conduction band, forming long-wave bands in the absorption spectra of the materials studied [5].

2. CALCULATION

2.1 The Structure Optimization

The electronic structure of ZnSeTe solid solutions doped with Fe atoms was calculated using the ABINIT complex of programs [6] in two stages.

* stepan.v.syrotiuk@lpnu.ua

At the first stage, structural optimization was done, which also consisted of two steps. The first step was to optimize the lattice parameter, and the second was to find the precise coordinates of the atoms of the supercell. In order to save space, we present the optimization results for the $Zn_4Se_2Te_2$ supercell, which contains eight atoms. The corresponding results are shown in

Table 1 – An example of optimizing the structure of a smaller supercell of a $Zn_4Se_2Te_2$ solid solution

Atom	*x*/*a*	*y*/*b*	*z*/*c*
Te	0.5	0	0
Te	0	0.5	0
Se	0	0	0.5
Se	0.5	0.5	0.5
Zn	0.75	0.25	0.2705
Zn	0.25	0.75	0.2705
Zn	0.25	0.25	0.7295
Zn	0.75	0.75	0.7295

As can be seen from Table 1, the Zn atoms have reduced z-coordinates (z/c) different from the starting ideal values 0.25, 0.25, 0.75, 0.75, respectively. The optimized values of the lattice lenghts have acquired the following values: $a = b = 11.27822$, $c = 11.26872$ a.u., respectively. The starting lattice lenghts had the same values $a = b = c = 11.12720$ a.u. For none of the atoms, the condition of fixing the reduced coordinates was not applied. And the lattice angles remained the same as in the ideal starting supercell, i.e. $\alpha = \beta = \gamma = 90$ degrees.

In this work, we performed all calculations for the $Zn_{31}Fe_1Se_{16}Te_{16}$ supercell, which consists of 64 atoms.

2.2 Details of the Calculation Scheme

Calculations of the electronic structure were performed here in the PAW basis (projector augmented waves) [7]. The PAW approach combines the properties of the pseudopotential (PP) [8] and the augmented plane wave (APW) [9] methods. Both of the latter methods use plane waves to calculate the matrix elements of the Hamiltonian operator.

In the PAW method, as in the APW approach, the crystal space consists of two parts: the augmentation space, which is inside the spheres built around the atoms, and the interspherical subspace (interstitial space). The augmentation spheres do not overlap, because the overlap can lead to numerical instability of the iterative searching for the wave functions of the crystal ground state. All components of the PAW basis are localized in these two subspaces [10].

The *first* component of the PAW basis $\tilde{\psi}$ is localized in the interspherical subspace, in which acts a weak pseudopotential. It corresponds to a smooth pseudowave function,

$$|\tilde{\psi}_{\boldsymbol{ak}}> = \sum_{\boldsymbol{G}} a(\boldsymbol{k}+\boldsymbol{G})|\,\boldsymbol{k}+\boldsymbol{G}>, \quad (1)$$

where $|\boldsymbol{k}+\boldsymbol{G}>$ are the plane waves, and $a(\boldsymbol{k}+\boldsymbol{G})$ are the Fourier series coefficients.

The *second* component of the PAW basis is localized in the deeper part of the augmentation sphere, in which are concentrated the atom core electrons and acts a strong atomic potential. The corresponding function is a linear combination of partial atomic waves ψ, i.e.

$$|\psi> \sum_i c_i \phi_i \quad .$$

The *third* component of the PAW basis is localized in the peripheral part of the augmentation sphere, in which acts a weak atomic pseudopotential, and the corresponding pseudowave function is a linear combination of partial atomic pseudowaves $\tilde{\psi}_i$, i.e.

$$|\tilde{\psi}> \sum_i c_i \tilde{\phi}_i. \quad (1)$$

In the PAW approach, a smooth pseudo-wave function $|\tilde{\psi}_{\boldsymbol{ak}}>$ is first calculated, from which the true all-electronic wave function $|\psi_{\boldsymbol{ak}}>$ is obtained. Here α is a band index, and $\boldsymbol{k}$ is a vector from the first Brillouin zone. The true all-electronic wave function is derived from the smooth pseudo-wave function using the operator τ [6]

$$|\psi_{\boldsymbol{ak}}> = \tau|\tilde{\psi}_{\boldsymbol{ak}}>, \quad (2)$$

which is constructed from partial atomic waves ψ, pseudowaves $\tilde{\psi}_i$ and projectors $\tilde{p}_i$, namely

$$\tau = 1 + \sum_i (|\varphi_i> - |\tilde{\varphi}_i>\,<\tilde{p}_i|, \quad (3)$$

The Schrödinger equation, which is based on the matrix of the Hamiltonian H, after replacing (2), (3) is reduced to the problem of the eigenfunctions and eigenvalues of the matrix of the effective Hamiltonian, with a mutual electronic energy spectrum $\varepsilon_{\boldsymbol{ak}}$, namely

$$\tau^+ H\tau|\tilde{\psi}_{\boldsymbol{ak}}> = \tau^+\tau|\tilde{\psi}_{\boldsymbol{ak}}> \varepsilon_{\boldsymbol{ak}}, \quad (4)$$

By means of the transformation τ, we obtain from the all-electronic Hamiltonian H an effective Hamiltonian $H_{eff} = \tilde{H} = \tau^+ H\tau$, the eigenfunction of which is called the pseudo-wave function $\tilde{\psi}_{\boldsymbol{ak}}$. From the latter, a true all-electronic function $\Psi_{\boldsymbol{ak}} = \tau\tilde{\psi}_{\boldsymbol{ak}}$ will be found. It allows us to calculate the dipole matrix elements necessary to obtain the optical constants of crystals and the kinetic coefficients of semiconductors [11].

The presence of a subsystem of strongly correlated 3d Fe electrons determines the use of a hybrid exchange-correlation functional. We chose the latter in the form of PBE0 [12], namely

$$E_{xc}^{PBE0}[\rho] = E_{xc}^{PBE}[\rho] + \beta(E_x^{HF}[\Psi_{3d}] - E_x^{PBE}[\rho_{3d}]), \quad (5)$$

In this functional, the exchange-correlation energy of the *3d* electrons of the Fe atom, found in the GGA [13] approximation, is partially removed, and the exchange energy of the same electrons, found in the Hartree-Fock theory, is substituted in its place. Namely, the PBE0 functional includes the usual PBE term, which corresponds to electrons with a smooth change in space of their density. The second term of formula (5) leads to the partial elimination of self-interaction error of 3d electrons. The mixing factor β is recommended to be 0.25 [12].

Previously, we tested and found the effectiveness of the exchange-correlation functional PBE0 for describing electronic subsystems that contain strongly correlated d-symmetry electrons. Various properties of semiconductors with impurities of *d* elements were investigated

using hybrid exchange-correlation functionals. In particular, the electronic structure of the crystal ZnS, doped with one or two transition metal atoms (Cr, Fe), was calculated [14]. It was also established the influence of cationic vacancies and hydrostatic pressure on electronic and magnetic properties of doped ZnTe:Mn crystal, with taking into consideration the strongly correlated 3d electrons [15]. The effect of the spin-orbit interaction on the electronic band energies in cadmium chalcogenides was revealed by means of the screened exchange energy, namely within the HSE_{06} – GW approach [16].

3. RESULTS AND DISCUSSION

The calculated electronic properties of the ZnSeTe solid solution, at ambient conditions, in which the Fe atom replaces the Zn atom, are shown in Figures 1-3. The external pressure equals to zero. As can be seen from Figures 1-3 the material ZnFeSeTe is a semiconductor for both spin orientations.

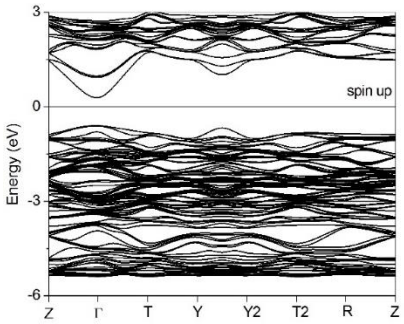

Fig. 1 – The majority-spin electronic energy bands, evaluated for supercell $Zn_{31}Fe_1Se_{16}Te_{16}$ at ambient conditions

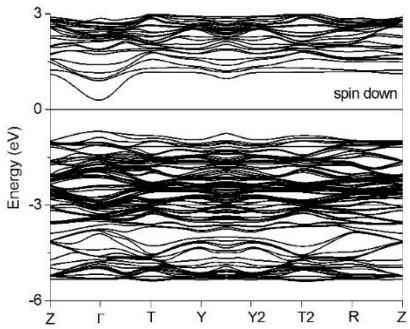

Fig. 2 – The minority-spin electronic energy bands, evaluated for supercell $Zn_{31}Fe_1Se_{16}Te_{16}$ at ambient conditions

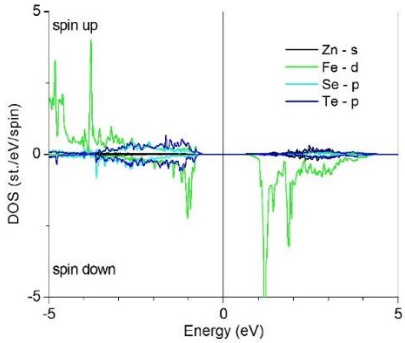

Fig. 3 – The majority- and majority-spin partial DOS, evaluated for supercell $Zn_{31}Fe_1Se_{16}Te_{16}$ at ambient conditions

The densities of states presented in Fig. 3 show that the top of the valence band is formed mainly by p states of Se and Te, as well as by d states of Fe.

Curves in Fig. 3 reveal a significant asymmetry of the Fe d states, which indicates the presence of a non-zero magnetic moment of the supercell. The latter equals to 4.0 μ_B and the Fe atom contribution is 3.23 μ_B.

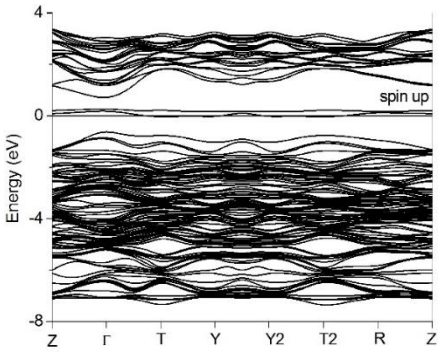

Fig. 4 – The majority-spin electronic energy bands, evaluated for supercell $Zn_{31}Fe_1Se_{16}Te_{16}$ at pressure 33 GPa

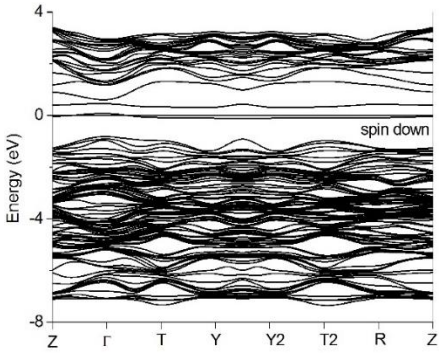

Fig. 5 – The minority-spin electronic energy bands, evaluated for supercell $Zn_{31}Fe_1Se_{16}Te_{16}$ at pressure 33 GPa

The results shown in Figures 4 – 6 allow us to reveal the effect of pressure on the electronic structure of the ZnFeSeTe material. The spin-polarized electron energy spectra shown in Figures 4, 5 reveal a metallic state at the Fermi level for electrons in spin-up and spin-down states, respectively.

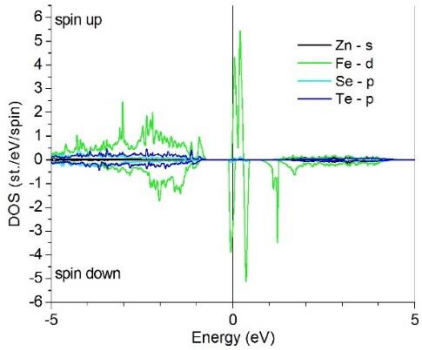

Fig. 6 – The majority- and majority-spin partial DOS, evaluated for supercell $Zn_{31}Fe_1Se_{16}Te_{16}$ at pressure 33 GPa

As can be seen from fig. 6, at the Fermi level dominate the Fe 3d electrons in spin-up and spin-down states. Narrow bands in which Fe 3d electrons move, as

well as large values of the density of states in them, indicate a subsystem of strongly correlated electrons. The most appropriate approach for describing such systems is the use of hybrid exchange-correlation energy functionals [12].

The total magnetic moment of the supercell under pressure 33 GPa equals to 0.78 μ_B and the contribution of the Fe atom dominates and amounts of 0.63 μ_B.

4. CONCLUSIONS

Electronic energy bands were calculated for $Zn_{31}Fe_1Se_{16}Te_{16}$ solid solution in which the Zn atom is replaced by the Fe atom. First, the optimized structural parameters of the solid solution were calculated, and then the electronic and magnetic properties of the material were evaluated. The specified properties were also found taking into account the external hydrostatic pressure. We found that at the pressure $P = 0$ the *3d* states of Fe are localized in both the valence and conduction bands. However, after application of hydrostatic pressure, namely $P = 33$ GPa, the dispersion curves of these electrons for both spin moment orientations cross the Fermi level. That is, the hydrostatic pressure causes an electronic semiconductor to metal phase transition. Therefore, in the absence of pressure, the considered material exhibited the properties of a ferromagnetically ordered semiconductor with a magnetic moment of 4 μ_B, and under the action of pressure $P = 33$ GPa, it turned out to be a magnetic metal with a supercell magnetic moment of 0.63 μ_B.

ACKNOWLEDGEMENTS

This contribution was created under the support of the High Performance Computing Laboratory at the Lviv Polytechnic National University.

REFERENCES

1. M. Yamamoto, A. Ebina, T. Takahashi, *Jpn. J. Appl. Phys.* **12**, 232 (1973).
2. C.-H. Su, S. Feth, S. Zhu, S.L. Lehoczky, L.J. Wang, *J. Appl. Phys.* **88**, 5148 (2000).
3. Y. Yang, Y. Hu, C. Liu, W. Li, J. Zhang, L. Wu, J. Yang, *Chalcogenide Letters*, **13**, 521 (2016).
4. S. Jagtapa, P. Chopadea, S. Tadepalli, A. Bhalerao, S. Gosavi, *Opto-Electron. Rev.* **27**, 90 (2019).
5. V.P. Makhniy, P.P. Horley, O.V. Kinzerskaya, E.V. Stets, *Appl. Opt.* **53**, B8 (2014).
6. X. Gonze, F. Jollet, F. Abreu Araujo, D. Adams, B. Amadon, T. Applencourt, C. Audouze, J.-M. Beuken, J. Bieder, A. Bokhanchuk, E. Bousquet, F. Bruneval, D. Caliste, M. Cote, F. Dahm, F. Da Pieve, M. Delaveau, M. Di Gennaro, B. Dorado, C. Espejo, G. Geneste, L. Genovese, A. Gerossier, M. Giantomassi, Y. Gillet, D.R. Hamann, L. He, G. Jomard, J. Laflamme Janssen, S. Le Roux, A. Levitt, A. Lherbier, F. Liu, I. Lukacevic, A. Martin, C. Martins, M.J.T. Oliveira, S. Ponce, Y. Pouillon, T. Rangel, G.-M. Rignanese, A.H. Romero, B. Rousseau, O. Rubel, A.A. Shukri, M. Stankovski, M. Torrent, M.J. Van Setten, B. Van Troeye, M.J. Verstraete, D. Waroquier, J. Wiktor, B. Xu, A. Zhou, J.W. Zwanziger, *Comput. Phys. Commun.* **205**, 106 (2016).
7. P.E. Blöchl, *Phys. Rev. B* **50**, 17953 (1994).
8. D. Vanderbilt, *Phys. Rev. B* **41**, 7892 (1990).
9. E. Sjöstedt, L. Nordström, D.J. Singh, *Solid State Commun.* **114**, 15 (2000).
10. A.R. Tackett, N.A.W. Holzwarth, G.E. Matthews, *Computer Phys. Comm.* **135**, 348 (2001).
11. O.P. Malyk, S.V. Syrotyuk, *J. Nano Electron. Phys.* **14**, 01014 (2022).
12. F. Tran, P. Blaha, K. Schwarz, P. Novák, *Phys. Rev. B* **74**, 155108 (2006).
13. J.P. Perdew, K. Burke, M. Ernzerhof, *Phys. Rev. Lett.* **77** 3865 (1996).
14. S.V. Syrotyuk, *J. Nano- Electron. Phys.* **13**, 05027 (2021).
15. S.V. Syrotyuk, *Acta Phys. Pol. A* **141**, 333 (2022).
16. S.V. Syrotyuk, O.P. Malyk, *J. Nano Electron. Phys.* **13**, 04003 (2021).

Вплив тиску на електронні та магнітні властивості твердого розчину ZnSeTe, легованого атомами Fe

S.V. Syrotyuk[1], M.K. Hussain[2]

[1] *Національний університет «Львівська політехніка», вул. С. Бандери, 12, 79013 Львів, Україна*
[2] *AL-Hussain University College, Karbala-Najaf str., 56001 Kerbala, Iraq*

У даній роботі розглядаються структурні характеристики утворення твердого розчину ZnSeTe. Після введення домішки заміщення Fe, були розраховані електронні енергетичні спектри та густини електронних станів. Виявлено суттєві зміни параметрів електронної структури та магнітних властивостей, зумовлені зовнішнім гідростатичним тиском. Установлено, що легований твердий розчин ZnFeSeTe за нормальних умов є напівпровідником для обох спінових орієнтацій. Однак під дією гідростатичного тиску цей матеріал переходить у металевий стан, оскільки 3d стани заліза тепер знаходяться на рівні Фермі. Під дією тиску магнітний момент суперелемента зменшується більш ніж у шість разів, тобто з 4,0 до 0,67 магнетона Бора.

Ключові слова: Твердий розчин ZnSeTe, Тривимірна домішка, Електронні енергетичні зони, Магнітний момент, Ефект тиску.